Possible production of cold plasmas through optical-field-induced ionization

S. C. Rae and K. Burnett
Clarendon Laboratory, Department of Physics, University of Oxford, Oxford OX1 3PU, United Kingdom
(Received 3 December 1991; revised manuscript received 11 May 1992)

A one-dimensional model incorporating Maxwell's equations and tunneling ionization is used to predict the plasma temperature after the passage of an intense femtosecond laser pulse through an atmospheric-density noble gas. These calculations are of relevance to a new class of proposed recombination x-ray lasers that use optical-field-induced ionization to generate an initially cold plasma. The residual plasma temperature is determined under a range of relevant conditions, and is found to be minimized for short laser pulses, short wavelengths, and the lowest intensity consistent with reaching the desired ionization stage. Even under optimum conditions, the predicted temperature is significantly greater than that required for high efficiency in the transient-gain regime.

PACS number(s): 52.50.Jm, 52.40.Db, 52.25.Jm, 42.55.Vc

I. INTRODUCTION

The amplification of spontaneous emission in a recombining plasma has been analyzed theoretically by many workers over the past 25 years, and comparatively recently x-ray gain has been observed in a range of systems, in which a suitably high recombination rate is obtained through adiabatic expansion or radiative cooling [1]. Gain has been measured on the $n=3\rightarrow 2$ transition in H-like ions, and the $n=5\rightarrow 3$ and $n=4\rightarrow 3$ transitions in Li-like ions. In these schemes, a quasi-steady-state population inversion is generated at a point in the cooling process where the upper level is still collisionally coupled to the levels above, but the lower level undergoes rapid radiative decay to the ground state. Transient gain on ground-state transitions is also theoretically achievable, if the ground state is initially sufficiently depopulated. The duration of this transient gain would be on the order of a radiative lifetime for the first excited state (~ 1 ps), much shorter than the duration of the quasi-steady-state gain, which is determined by the plasma cooling time (0.1–1 ns).

Plasmas produced by optical-field-induced ionization (OFI) have certain desirable properties for recombination x-ray laser schemes. The pulse duration produced by the latest generation of intense lasers is sufficiently short to allow the possibility of transient gain on ground-state transitions and, more importantly, the residual plasma temperature may be low enough to allow rapid recombination to commence without the need for additional cooling. In a collision-dominated plasma, rapid ionization only occurs if the average electron energy is significantly greater than the ionization potential. However, in an OFI plasma the strength of the optical field alone determines the ionization rate, and the temperature can be considerably lower. Recent theoretical studies by Burnett and Enright [2] and Amendt, Eder, and Wilks [3] have proposed various OFI x-ray laser schemes. The plasma temperature is a crucial parameter in determining the feasibility and potential energy efficiency of such schemes. In this paper we develop a one-dimensional (1D) computer model in order to calculate the plasma temperature for the case of an intense femtosecond laser pulse propagating through an atmospheric-density noble gas.

In Sec. II we discuss some of the mechanisms which can contribute to the heating of an OFI plasma and present qualitative estimates of above-threshold-ionization energy and collisional heating. The 1D propagation-ionization model is outlined in Sec. III, and calculations of the plasma temperature are presented in Sec. IV. We examine the implications of these results for a potential OFI x-ray laser scheme in Sec. V. The results concentrate on a neon plasma, and are thus directly relevant to the proposal by Amendt, Eder, and Wilks [3] for a recombination x-ray laser in the transient-gain regime in Li-like Ne.

II. PLASMA HEATING

Various processes can lead to the heating of OFI plasmas, including above-threshold-ionization (ATI) energy, collisional heating (nonlinear inverse bremsstrahlung), stimulated Raman or Compton scattering, and space-charge or plasma oscillations. In this paper, only the effects of the first two mechanisms, ATI and collisional heating, will be calculated in detail.

The most fundamental of these processes is the ATI energy arising during the field-induced-ionization process. In the high-intensity limit this has a simple classical explanation [4]. Electrons which are ionized at a point in the laser cycle displaced from the peak acquire a dephasing energy, and this appears as residual kinetic energy once the pulse has passed. For a linearly polarized sinusoidal field, an electron ionized at time t_0 will have an average kinetic energy of

$$\tfrac{1}{2}m_e\langle v^2\rangle=\frac{e^2E_0^2}{4m_e\omega_0^2}(1+2\cos^2\omega_0 t_0)\ , \tag{1}$$

where E_0 is the amplitude of the electric field and ω_0 is the laser angular frequency. The first term in this expression is the coherent quiver energy $\mathcal{E}_q$, and the second

term is the dephasing or ATI energy. Integrating over a laser cycle, the average ATI energy can be written

$$\mathcal{E}_{\mathrm{ATI}}=\frac{2\mathcal{E}_q\int\mathcal{R}(\phi)\cos^2\phi\,d\phi}{\int\mathcal{R}(\phi)d\phi}\ , \tag{2}$$

where $\mathcal{R}(\phi)$ is the ionization rate, and ϕ is the phase of the field.

For a high-intensity laser pulse, ionization can be calculated using the generalized tunneling formula due to Ammosov, Delone, and Krainov [5], based on earlier work by Perelomov, Popov, and Terentev [6]. The static-field ionization rate is given by

$$\mathcal{R}_{\mathrm{st}}=\frac{\omega_{\mathrm{at}}}{2}C_{n^*}^2\frac{\mathcal{E}_i}{\mathcal{E}_h}\frac{(2l+1)(l+|m|)!}{2^{|m|}(|m|)!(l-|m|)!}\times\left[2\left[\frac{\mathcal{E}_i}{\mathcal{E}_h}\right]^{3/2}\frac{E_{\mathrm{at}}}{E}\right]^{2n^*-|m|-1}\times\exp\left[-\frac{2}{3}\left[\frac{\mathcal{E}_i}{\mathcal{E}_h}\right]^{3/2}\frac{E_{\mathrm{at}}}{E}\right]\ . \tag{3}$$

Here E is the instantaneous electric field, $\mathcal{E}_i$ is the ionization potential for the atom or ion concerned, $\mathcal{E}_h$ is the ionization potential for hydrogen, ω_{at} and E_{at} are the atomic units for frequency and electric field, l and m are quantum numbers for the initial state, $n^*=Z(\mathcal{E}_h/\mathcal{E}_i)^{1/2}$ is the effective principle quantum number, and $C_{n^*}\simeq(2\varepsilon/n^*)^{n^*}(2\pi n^*)^{-1/2}$ is a constant of order unity. This equation can be averaged over an optical cycle to obtain the mean ionization rate in a sinusoidal field,

$$\mathcal{R}=\left[\frac{3}{\pi}\frac{E}{E_{\mathrm{at}}}\left[\frac{\mathcal{E}_h}{\mathcal{E}_i}\right]^{3/2}\right]^{1/2}\mathcal{R}_{\mathrm{st}}\ . \tag{4}$$

Recent experiments [7] have confirmed that the generalized tunneling formula is in generally good agreement with observations. Overall, the formula predicts the appearance intensities of various ion stages within a factor of 2, and certainly performs better than the standard Keldysh model for higher charge states.

The ATI energy of electrons produced in a realistic situation depends on the intensity at which ionization occurs. Figure 1(a) shows the cycle-averaged tunneling ionization rate [from Eq. (4)] as a function of intensity, for a number of ionization stages of neon. A dashed line marks the intensity at which each rate reaches 10^{15} s^{-1}, which can be used as an approximate appearance intensity. In Fig. 1(b) the average ATI energy for each stage [from Eq. (2)] is shown as a function of laser intensity, for a laser wavelength of 248 nm. The dashed lines from Fig. 1(a) are extended in order to find the ATI energy at the appearance intensity (listed in Table I). The ATI energy increases from a few electron volts for Ne^+ to nearly 200 eV for Ne^{8+}, and the ratio of the ATI energy to the ionization potential increases with the ionization stage, but always remains less than unity. For a potential x-ray laser scheme, it is obviously the electrons from the highest ionization stages which contribute most to the final plasma temperature. The ATI energy can only be

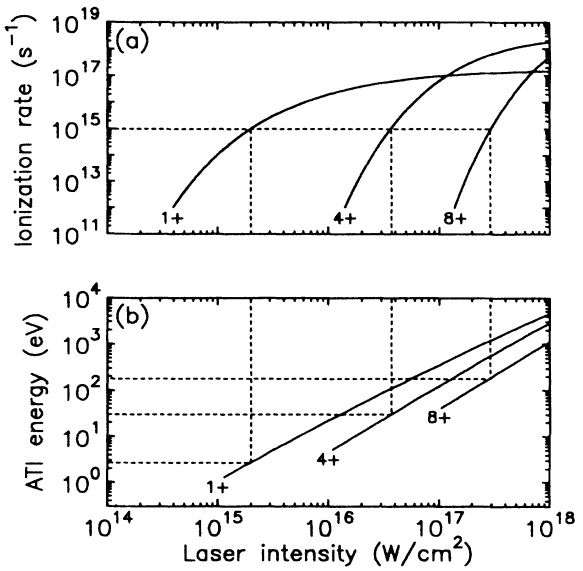

FIG. 1. (a) Cycle-averaged tunneling ionization rates for a number of ionization stages of neon; (b) ATI energy as a function of laser intensity.

reduced by using a shorter laser wavelength (to minimize the coherent quiver energy), or by increasing the pulse length (to lower the effective appearance intensity). For the conditions of Fig. 1, a plasma stripped to Ne^{8+} would have an average ATI energy of around 75 eV.

The proposed OFI x-ray laser schemes require electron densities on the order of 10^{20} cm^{-3}, and at these densities collisional heating (nonlinear inverse bremsstrahlung) will also play an important role. The effect of electron-ion collisions is to perturb the coherent oscillatory motion of the electrons and transfer a fraction of the quiver energy into random thermal motion. For a velocity-independent electron-ion collision frequency ν_{ei}, and assuming $\nu_{\mathrm{ei}}\ll\omega_0$, the cycle-averaged power absorption per electron is given by [8]

$$P=\frac{e^2E_0^2\nu_{\mathrm{ei}}}{2m_e\omega_0^2}\ . \tag{5}$$

For a gaseous plasma at a temperature of greater than a few electron volts (in the classical weakly coupled regime), the Spitzer expression for the collision frequency is valid. Assuming a Maxwellian velocity distribution, this is given by [9,10]

$$\nu_{\mathrm{ei}}=\frac{4\sqrt{2\pi}}{3}\frac{Zn_ee^4\ln\Lambda}{(4\pi\epsilon_0)^2m_e^{1/2}(k_BT_e)^{3/2}}\ , \tag{6}$$

where Z is the degree of ionization, T_e is the electron temperature, and $\ln\Lambda$ is the Coulomb logarithm, defined in the usual way. At high laser intensities, a correction for the electron quiver motion needs to be included, and the expression becomes nonlinear. An approximate collision frequency in this regime can be obtained by multiplying the Spitzer expression by a factor [11]

$$F=(1+v_q^2/3v_{\mathrm{th}}^2)^{-3/2}\ . \tag{7}$$

TABLE I. Appearance intensity for a number of ionization stages of neon, the quiver energy at this intensity, and the residual ATI energy, calculated for 248-nm light.

Ionization stage	Ionization potential (eV)	Appearance intensity (W/cm^2)	Quiver energy (eV)	ATI energy (eV)	Fraction of ionization potential
Ne^+	21.6	2.0×10^{15}	11.6	2.7	0.13
Ne^{4+}	97.1	3.7×10^{16}	214	30	0.31
Ne^{8+}	239.1	2.9×10^{17}	1680	180	0.75

Here $v_{th}=(k_BT_e/m_e)^{1/2}$ is the characteristic thermal velocity and $v_q=eE_0/m_e\omega_0$ is the quiver velocity.

Using Eqs. (5)–(7), the collisional heating rate for a given set of plasma conditions can be estimated. This heating rate is plotted in Fig. 2 as a function of laser intensity, for $n_e=10^{20}$ cm^{-3}, $Z=8$, and $\lambda_0=248$ nm. Curves are shown for three different electron temperatures: $k_BT_e=10$, 30, and 100 eV. At low intensities the heating rate is linear in the laser intensity, and is a sensitive function of the plasma temperature. Above about 10^{16} W/cm^2 the heating rate decreases with intensity, and in this region, where the quiver energy is large compared with the thermal energy, the heating rate is roughly independent of the plasma temperature. For the conditions of Fig. 2 at a laser intensity of 10^{17} W/cm^2, the collisional heating rate is approximately 800 eV/ps.

The two mechanisms discussed above, ATI and collisional heating, set a lower bound on the plasma temperature which is achievable in any proposed OFI x-ray laser scheme. Further collective effects, such as stimulated Raman scattering, Compton scattering, and space-charge oscillations, will in general act to increase the plasma temperature further. Thus it is of considerable importance that a detailed calculation be made of the temperature contribution from ATI and collisions under a wide range of conditions. Burnett and Enright [2] rely on simple estimates (along the lines of Figs. 1 and 2) to assess the feasibility of a number of x-ray laser schemes, while Amendt, Eder, and Wilks [3] use the recent calculations of Penetrante and Bardsley [12]. This latter work, based on 1D particle-in-cell (PIC) simulations, suggests that under realistic conditions (248 nm, 100 fs, 10^{17} W/cm^2 laser pulse, electron density $\sim10^{20}$ cm^{-3}), highly stripped plasmas can be produced with temperatures as low as

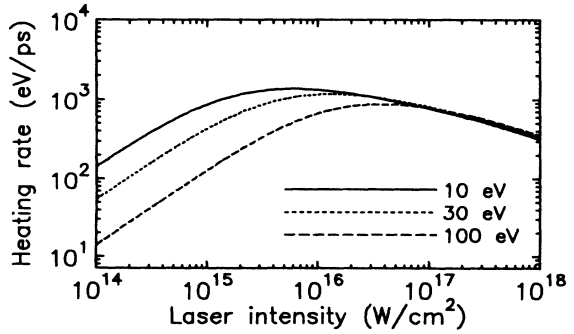

FIG. 2. Collisional heating rate as a function of laser intensity for $n_e=10^{20}$ cm^{-3}, $Z=8$, and $\lambda_0=248$ nm.

10–20 eV. To complement this, Amendt, Eder, and Wilks present results from 2D PIC simulations which show that the additional heating from stimulated Raman scattering can also be kept to tolerable levels ($\lesssim 50$ eV) by carefully controlling the laser-pulse length and electron density.

With the model to be outlined below, we aim to provide an accurate calculation of the ATI energy and collisional heating, using an alternative technique to that used by Penetrante and Bardsley. A comparison between the predictions using the two different models will be given in a subsequent section.

III. PROPAGATION-IONIZATION MODEL

In our model we assume a 1D plasma, and solve a coupled set of rate equations at each point simultaneously with Maxwell's equations for the propagation of a linearly polarized laser pulse [13]. Ionization is calculated using the static-field form of the tunneling expression Eq. (3). This ions are assumed to be in their ground states, and only sequential ionization processes are considered. The populations of the various ionization stages as functions of time are then obtained from a set of coupled first-order differential equations of the form

$$\frac{dN_k}{dt}=-\mathcal{R}_kN_k+\mathcal{R}_{k-1}N_{k-1}\ , \tag{8}$$

where $\mathcal{R}_k$ is the ionization rate and N_k the population of the kth stage.

In 1D, a transverse electromagnetic pulse obeys the time-dependent wave equation

$$\frac{\partial^2E}{\partial x^2}-\frac{1}{c^2}\frac{\partial^2E}{\partial t^2}-\mu_0\frac{\partial J}{\partial t}=0\ , \tag{9}$$

where J is the total plasma current. The current is calculated from the electron distribution function,

$$J(x,t)=-e\int f_e(x,v,t)v\,dv\ , \tag{10}$$

and the evolution of this distribution function is governed, in general, by a Boltzmann equation,

$$\frac{\partial f_e}{\partial t}+v\frac{\partial f_e}{\partial r}-\frac{eE}{m_e}\frac{\partial f_e}{\partial v}=\mathcal{C}(f)+\mathcal{S}(f)\ , \tag{11}$$

where $\mathcal{S}(f)$ is a source term (from OFI, via the coupled rate equations) and $\mathcal{C}(f)$ is the collision integral. Note that effects due to the magnetic field are neglected here, which assumes nonrelativistic behavior, $v_q\ll c$. For

248-nm laser light, this limits the intensity to $I \ll 2.2\times10^{19}$ W/cm^2.

Instead of numerically solving the complete Boltzmann equation, we make some simplifications to Eq. (11) to improve the efficiency of the calculations. The electrons are constrained to move perpendicular to the direction of propagation, and are assumed to oscillate coherently in the laser field. This allows us to define a distribution-averaged velocity $\bar{v}(x,t)$, and include the effect of the laser field by solving the equation of motion for this average velocity. Effectively we work in a frame of reference which moves with the quiver oscillations. A major benefit of this change is that the average ATI energy can be calculated at any point in time by simply taking the appropriate moment of the distribution function,

$$\mathcal{E}_{\rm ATI}(x,t)=\frac{\int (1/2)m_e v^2 f_e(x,v,t)dv}{\int f_e(x,v,t)dv} . \tag{12}$$

Collisional heating is incorporated by modifying the equation of motion for the velocity to include a friction term,

$$\frac{\partial \bar{v}}{\partial t}+\nu_{\rm ei}\bar{v}=\frac{-eE}{m_e} . \tag{13}$$

The instantaneous power absorption per electron as a function of distance is then given by

$$P(x,t)=\frac{\int m_e \nu_{\rm ei} v^2 f_e(x,v,t)dv}{\int f_e(x,v,t)dv} . \tag{14}$$

The electron-ion collision frequency $\nu_{\rm ei}=\nu_{ei}(\bar{v})$ is determined using the Spitzer expression for a straight-line velocity [9,10],

$$\nu_{\rm ei}=\frac{8\pi Z n_e e^4 \ln\Lambda}{(4\pi\epsilon_0)^2 m_e^2 \bar{v}^3} . \tag{15}$$

This is valid in the limit where the instantaneous velocity is much greater than the thermal velocity. At the intensities required for the production of Ne^{8+} the quiver energy is greater than 1 keV (see Table I), so this approximation holds over much of the laser cycle. Where the instantaneous velocity becomes less than the thermal velocity, a correction is made to Eq. (15) which results in a correct reduction to the Spitzer expression for a Maxwellian distribution, Eq. (6), in the appropriate limit. The ATI electron energy distribution is not Maxwellian, and although electron-electron collisions (not included in the present model) would eventually thermalize the population, the equilibration rate is not always rapid compared with the duration of the pulse [14]. For $n_e=10^{20}$ cm^{-3} and $k_B T_e=20$ eV, the equilibration time τ_{ee} is 40 fs, and this time scales as $\tau_{ee}\propto(k_B T_e)^{3/2} n_e^{-1/2}$. Even if the distribution is not Maxwellian, however, an effective ATI temperature can be defined through $k_B T_{\rm ATI}=\frac{2}{3}\mathcal{E}_{\rm ATI}$. A minimum temperature must be assumed for the Spitzer expression to remain valid, and this is typically taken as 5 eV. As long as the final temperature is significantly greater than this imposed minimum, the actual choice is not critical.

Langdon [15] has shown that there may be a reduction of up to ~50% in the effective collision frequency arising from a non-Maxwellian electron distribution. This will undoubtedly have some effect here, but there is no simple way in which to incorporate the modification. The correction originally proposed by Langdon is only valid in the regime where $Zv_q \gtrsim v_{\rm th}$ and $v_q \ll v_{\rm th}$, and our model deals with significantly higher intensities. We can at least state that the present method of calculation gives an upper limit on the temperature produced by collisional heating.

Finally, to ensure energy conservation during ionization, an extra term is added to the plasma current,

$$J=-e\int f_e(x,v,t)v\,dv+J_{\rm ioniz} . \tag{16}$$

The ionization current $J_{\rm ioniz}$ is obtained by equating the energy loss through ionization to the Joule heating,

$$EJ_{\rm ioniz}=\sum_k \mathcal{R}_k N_k \mathcal{E}_k . \tag{17}$$

The complete system of equations was solved numerically using an explicit finite-difference technique [16].

IV. RESULTS

The results in this section all refer to a neon plasma, and a laser pulse with a sine-squared field envelope (pulse durations given are full width at half maximum). The length of the plasma in each case is $20\lambda_0$, where λ_0 is the vacuum laser wavelength. Over such a relatively short length, the pulse does not lose a significant amount of energy, and the conditions in the plasma after the passage of the pulse are almost constant. Thus, in general, we plot only spatial averages of the final plasma conditions.

Figure 3 shows the final plasma temperature and degree of ionization as functions of the peak laser intensity,

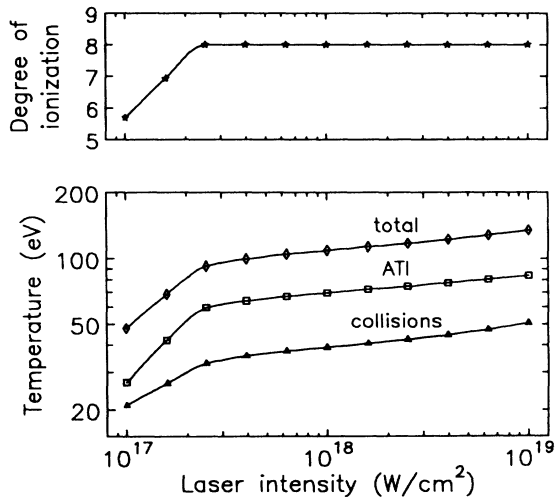

FIG. 3. Plasma temperature and final degree of ionization as functions of laser intensity, for a 248-nm, 100-fs laser pulse and a Ne atom density of 2.5×10^{18} cm^{-3}.

for a 248-nm, 100-fs laser pulse and a gas density of 2.5×10^{18} cm^{-3}. The minimum intensity required for the production of a Ne^{8+} plasma is $\sim2.5\times10^{17}$ W/cm^2, and further calculations, not shown here, confirm that this is independent of the plasma density.

At intensities below the critical intensity, the dependence of temperature on intensity is difficult to analyze, as there is the added complication of a varying degree of ionization, but above this point the behavior is somewhat easier to interpret. The ATI temperature increases slowly, approximately as $I^{0.1}$, above the critical intensity. If ionization of a particular stage always occurred at some fixed appearance intensity, the ATI temperature would be independent of the peak pulse intensity, but the fact that it has a small positive slope indicates that this is not quite the case. In a femtosecond laser pulse, the intensity rise time is comparable with the ionization rates, and increasing the peak intensity allows each of the ionization stages to survive to a slightly higher intermediate intensity.

In the high-intensity limit, where the quiver energy is much larger than the thermal energy, the electron-ion collision frequency would decrease as $I^{-3/2}$, and the collisional heating rate would decrease as $I^{-1/2}$. The collisional temperature in Fig. 3, however, shows a small positive slope. This is partly because some of the absorption (in the edges of the pulse) does not occur in the high-intensity regime, and also because at higher intensities the electron density rises to its maximum value earlier in the pulse, increasing the total absorption.

The two heating mechanisms considered, ATI and electron-ion collisions, show quite different time-dependent behavior. This is illustrated in Fig. 4, which plots the degree of ionization and the temperature contributions from ATI and collisions as functions of time, for a typical element of the plasma. The laser wavelength is 248 nm, peak intensity 2.5×10^{17} W/cm^2, pulse duration 100 fs, and gas density 1.25×10^{19} cm^{-3}. The final ionization state is Ne^{8+} (electron density $n_e=10^{20}$ cm^{-3}), and virtually all the ionization occurs in the leading edge of the pulse. The ATI contribution is seen to follow the steps in the ionization, reaching a plateau of 60 eV at the peak of the pulse. The collisional contribution is less important early in the pulse, but the gradient steepens and

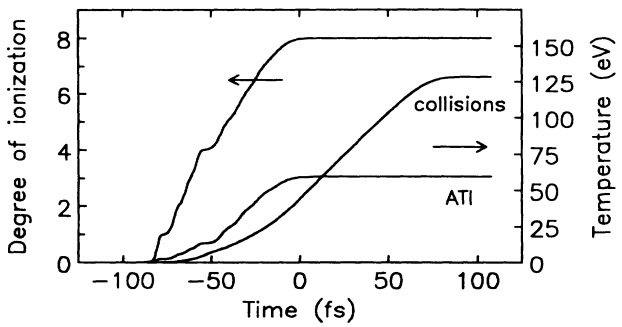

FIG. 4. Time dependence of the degree of ionization and the contributions to the plasma temperature in a Ne plasma, for a 248-nm, 100-fs, 2.5×10^{17} W/cm^2 laser pulse, and a final electron density of 10^{20} cm^{-3}.

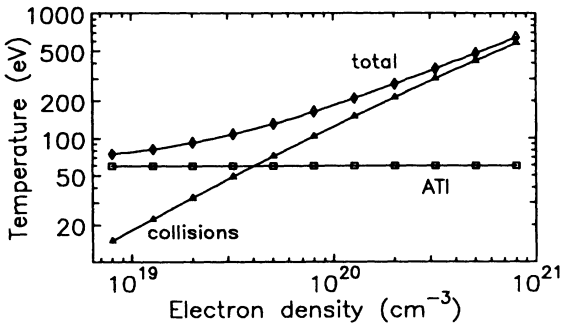

FIG. 5. Plasma temperature as a function of electron density in a Ne^{8+} plasma, for a 248-nm, 100-fs, 2.5×10^{17}-W/cm^2 laser pulse.

heating continues right across the pulse to reach a final value of about 125 eV. The collisional heating rate remains almost constant during the trailing edge of the pulse; although the intensity is decreasing, the effective collision rate is increasing (see Fig. 2).

Figure 5 shows the variation in plasma temperature with density, for a 248-nm, 100-fs laser pulse at the minimum intensity required for producing a Ne^{8+} plasma, 2.5×10^{17} W/cm^2. The ATI temperature, as expected, is independent of the plasma density. The collisional temperature increases almost exactly linearly with density, in accordance with the density dependence of the collision frequency.

Short pulses are favorable to the production of cold plasmas, as shown in Fig. 6, for a 248-nm laser pulse at an intensity of 2.5×10^{17} W/cm^2 and a gas density of 2.5×10^{18} cm^{-3}. The ATI temperature is determined by the intensity at which the various intermediate stages are ionized. If the field-induced ionization rates were infinitely fast above some threshold intensity, then complete ionization of a particular stage would always occur at a fixed appearance intensity, and the ATI temperature would be independent of the pulse duration. This would apply in the long-pulse limit $\tau\gg100$ fs. However, for short pulses the ionization rates cannot be considered to be infinitely fast; the populations of the various ionization stages do not have sufficient time to come to equilibrium, and as the pulse becomes shorter, intermediate ionization stages survive to higher intensities. The ATI temperature

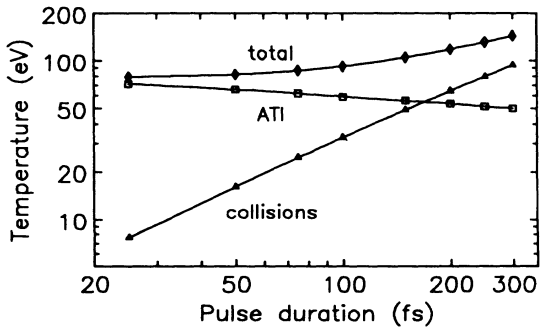

FIG. 6. Plasma temperature as a function of pulse duration, for a 248-nm, 2.5×10^{17}-W/cm^2 laser pulse and a Ne atom density of 2.5×10^{18} cm^{-3}.

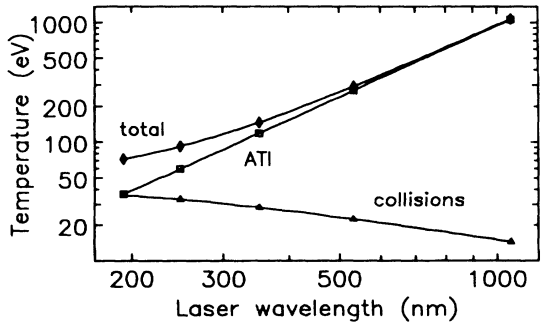

FIG. 7. Plasma temperature as a function of laser wavelength, for a 100-fs, 2.5×10^{17}-W/cm^2 laser pulse and a Ne atom density of 2.5×10^{18} cm^{-3}.

thus increases slightly as the pulse duration is reduced. For the very shortest pulses, the final stage is not even completely ionized. The collisional temperature increases almost exactly linearly with increasing pulse duration, and as the total plasma temperature is dominated by the collisional component, shorter pulses reduce the total temperature.

The plasma temperature as a function of laser wavelength is shown in Fig. 7, for a 100-fs laser pulse at a peak intensity of 2.5×10^{17} W/cm^2 and a gas density of 2.5×10^{18} cm^{-3}. The ATI temperature increases almost exactly as λ_0^2, proportional to the increase in the quiver energy. The collisional temperature decreases slowly with increasing laser wavelength. In the high-intensity limit, where $\nu_{ei}\propto\mathcal{E}_q^{-3/2}$, the collisional absorption rate would be expected to decrease as λ_0^{-1}. The proportionality here is closer to $\lambda_0^{-1/2}$, and this difference is probably caused by collisional heating near the ends of the laser pulse, where the high-intensity limit does not apply. Overall, the reduction in the ATI temperature for shorter wavelengths is more significant than the increase in the collisional temperature, and the total plasma temperature decreases.

V. DISCUSSION

The optimum conditions for producing cold plasmas by OFI are short laser wavelength, short pulse duration, and an intensity just sufficient to reach the desired ionization stage. For the specific case of Ne^{8+}, and a 248-nm, 100-fs laser pulse, the minimum intensity required is 2.5×10^{17} W/cm^2. At this intensity, the contribution to the final plasma temperature from ATI is approximately 60 eV (independent of the density), and the total temperature as a function of electron density is given in Fig. 5. The proposed recombination x-ray laser scheme of Amendt, Eder, and Wilks [3] requires an electron density of $\gtrsim10^{20}$ cm^{-3} and a total plasma temperature of $\lesssim50$ eV for large gain and high overall efficiency. For $n_e=10^{20}$ cm^{-3}, our model predicts a total plasma temperature of 185 eV, of which approximately 60 eV is due to ATI and 125 eV due to collisional heating. Note that this does not take into account additional contributions from Raman heating or other collective mechanisms, which will raise the temperature further. The x-ray gain in a recombining plasma is an extremely sensitive function of temperature, and unless some way is found to significantly reduce both the ATI and collisional contributions, this result suggests that the Li-like Ne scheme is only marginally feasible.

The temperatures obtained from our model do not agree with those calculated under similar conditions by Penetrante and Bardsley [12], who find that for a 248-nm, 200-fs laser pulse at an intensity of 10^{18} W/cm^2, and a Ne^{8+} plasma at an electron density of 10^{20} cm^{-3}, the ATI temperature is around 10 eV. In addition, they find that collisional heating has only a minimal additional effect. Under similar conditions, our model predicts a total plasma temperature of around 200 eV, a large part of which results from collisional heating. Penetrante and Bardsley attribute the extremely low temperatures to a matching of the laser-pulse duration with the strength of the space-charge field. However, for the laser intensities and plasma densities of interest, the PIC code results presented in the same study show no cavitation, hence no charge separation. If there is a strong space-charge effect, it would be expected to depend strongly on the size of the focal spot, but such a dependence is not reported. In addition, recent work by Leemans *et al.* [17] suggests that including space-charge effects leads to an increased, not decreased, plasma temperature. We acknowledge that space charge does play a role in determining the plasma temperature, one which we cannot address with our model, but we believe that the contributions from ATI and collisional heating are fundamental and important in their own right.

Aside from the issue of plasma heating, it may also prove to be difficult to actually produce a long filament of highly ionized gas. For the transient-gain regime, where the gain duration is on the order of 1 ps, a traveling-wave pump geometry will be necessary. In their proposal, Amendt, Eder, and Wilks [3] assume a focal spot half-intensity radius of typically 5–30 μm. This corresponds to a confocal parameter of up to several centimeters, and focusing an intense laser pulse through a rapidly ionizing medium over such a long distance is by no means a trivial task. Defocusing caused by the rapid ionization would tend to disrupt the propagation of a Gaussian beam over much shorter distances. Leemans *et al.* [17] have shown that ionization-induced defocusing can act to clamp the maximum density achievable in a tight laser focus. A number of studies have been published recently concerning self-channeling of laser pulses and the formation of plasma waveguides [18–23], but these have largely dealt with the problem of an intense pulse propagating through a preformed plasma. We are currently working on extending our model to allow the investigation of defocusing effects during the plasma formation process.

ACKNOWLEDGMENT

This work is part of a program supported by the Science and Engineering Research Council.

[1] For a review of the theory and experiments relating to recombination x-ray lasers, see R. C. Elton, *X-Ray Lasers* (Academic, San Diego, 1990); and *X-Ray Lasers,* edited by G. Tallents (IOP, Bristol, 1991).

[2] N. H. Burnett and G. D. Enright, IEEE J. Quantum Electron. **26**, 1797 (1990).

[3] P. Amendt, D. C. Eder, and S. C. Wilks, Phys. Rev. Lett. **66**, 2589 (1991); D. C. Eder, P. Amendt, and S. C. Wilks, Phys. Rev. A **45**, 6761 (1992).

[4] N. H. Burnett and P. B. Corkum, J. Opt. Soc. Am. B **6**, 1195 (1989).

[5] M. V. Ammosov, N. B. Delone, and V. P. Krainov, Zh. Eksp. Teor. Fiz. **91**, 2008 (1986) [Sov. Phys.—JETP **64**, 1191 (1987)].

[6] A. M. Perelomov, V. S. Popov, and M. V. Terentev, Zh. Eksp. Teor. Fiz. **50**, 1393 (1966) [Sov. Phys.—JETP **23**, 924 (1966)].

[7] S. Augst, D. D. Meyerhofer, D. Strickland, and S. L. Chin, J. Opt. Soc. Am. B **8**, 858 (1991).

[8] T. P. Hughes, *Plasmas and Laser Light* (IOP, Bristol, 1975).

[9] L. Spitzer, Jr., *Physics of Fully Ionized Gases,* 2nd ed. (Interscience, New York, 1962), Chap. 5.

[10] I. P. Shkarofsky, T. W. Johnston, and M. P. Bachynski, *The Particle Kinetics of Plasmas* (Addison-Wesley, Reading, MA, 1966), Chap. 7.

[11] L. Schlessinger and J. Wright, Phys. Rev. A **20**, 1934 (1979).

[12] B. M. Penetrante and J. N. Bardsley, Phys. Rev. A **43**, 3100 (1991).

[13] This model is very similar to that used previously in simulations of plasma-induced spectral blueshifting [S. C. Rae and K. Burnett, Phys. Rev. A **46**, 1084 (1992)]. However, in the present case the spectrum is of secondary importance to the plasma heating.

[14] R. A. Cairns, *Plasma Physics* (Blackie, Glasgow, 1985), Chap. 3.

[15] A. B. Langdon, Phys. Rev. Lett. **44**, 575 (1980).

[16] W. H. Press, B. P. Flannery, S. A. Teukolsky, and W. T. Vetterling, *Numerical Recipes: The Art of Scientific Computing* (Cambridge University Press, Cambridge, England, 1986).

[17] W. P. Leemans, C. E. Clayton, W. B. Mori, K. A. Marsh, A. Dyson, and C. Joshi, Phys. Rev. Lett. **68**, 321 (1992).

[18] G. Z. Sun, E. Ott, Y. C. Lee, and P. Guzdar, Phys. Fluids **30**, 526 (1987).

[19] W. B. Mori, C. Joshi, J. M. Dawson, D. W. Forslund, and J. M. Kindel, Phys. Rev. Lett. **60**, 1298 (1988).

[20] J. C. Solem, T. S. Luk, K. Boyer, and C. K. Rhodes, IEEE J. Quantum Electron. **25**, 2423 (1989).

[21] T. Kurki-Suonio, P. J. Morrison, and T. Tajima, Phys. Rev. A **40**, 3230 (1989).

[22] P. Sprangle, E. Esarey, and A. Ting, Phys. Rev. A **41**, 4463 (1990).

[23] R. Rankin, C. E. Capjack, N. H. Burnett, and P. B. Corkum, Opt. Lett. **16**, 835 (1991).